In situ generation of ZnO nanoparticles within a polyethyleneimine matrix for antibacterial zein fibres

Leno Mascia[1], Wanwei Zhang[1], Francesca Gatto[2], Alice Scarpellini[3], Pier Paolo Pompa[2] and Elisa Mele[1]*

[1] *Department of Materials, Loughborough University LE11 3TU, UK*

[2] *Nanobiointeractions and Nanodiagnostics, Istituto Italiano di Tecnologia, via Morego 30, 16163 Genoa, Italy*

[3] *Electron Microscopy Facility, Istituto Italiano di Tecnologia, via Morego 30, Genova 16163, Italy*

*Corresponding author: e.mele2@lboro.ac.uk

Abstract

In this study the potential of branched polyethyleneimine (PEI) was explored for the *in-situ* generation of ZnO nanoparticles and the electrospinning of zein-based fibres. Zinc acetyl acetonate dihydrate ($ZnAcAc \cdot 2H_2O$) was chosen as the precursor for the related sol-gel reactions, leading to the nucleation and growth of wurtzite crystals within the PEI matrix. Control experiments showed that PEI played a vital role in the reaction steps leading to the conversion. Wide angle X-ray diffraction analysis confirmed the crystallographic structure of the ZnO particles formed, while scanning electron microscopy examinations revealed the formation of agglomerates less than 400 nm, made up of much smaller primary nanoparticles. The obtained ZnO/PEI micro-suspensions in ethanol were mixed in an ethanol/water solution of zein and used for electrospinning of different types of zein-modified fibres. Differential scanning calorimetry analysis showed that PEI acted as a plasticizer for zein, causing also a broadening of the glass transition, while Fourier-transform infrared spectroscopy indicated that the amine groups in PEI interacted with the surface groups of ZnO crystals. The results provide useful insights for formulating fibres, films and coatings exhibiting antibacterial characteristics, as well as higher mechanical flexibility and toughness relative to plain zein.

Keywords: Electrospinning, Polyethyleneimine, Zein, Zinc acetylacetonate, Zinc oxide

1. Introduction

Zein is found in the endosperm of corn and belongs to the group of storage proteins known as prolamins, which are the main repository for nitrogen in cereal seeds.[1] Zein mainly contains nonpolar amino acids, such as leucine, proline and alanine. The lack of polarity arises from the dipole cancellation effect of the constituent amine and acid groups through internal associations, which determine the hydrophobic character and poor water solubility of this protein.[1, 2] For this reason, ethanol or alkaline solutions are used to process zein from "stocks" of solutions or dopes.

Biocompatibility, biodegradability and processing versatility for a wide range of products, such as films, nanoparticles and nanofibres, make zein a material of interest for biomedical applications, particularly for tissue engineering and drug delivery.[3] According to Zhang *et al.,* zein was approved as a "generally recognized as safe" (GRAS) excipient in 1985 by the United States Food and Drug Administration (FDA) for film coating of pharmaceuticals.[4] Zein-based nanofibres have been produced by electrospinning from alcoholic solutions and have also been proposed for the release of antibacterial compounds and drugs,[5, 6] such as eucalyptus essential oil,[7] gallic acid,[8] curcumin,[9] indomethacin,[10] aceclofenac[11] and silver,[12] and for promoting skin regeneration.[13-16] Moreover, bio-functional nanoparticles or other biopolymers have been added to electrospun zein nanofibres. Babitha and Korrapati have incorporated TiO_2 nanoparticles in zein and polydopamine (PDA) nanofibrous scaffolds.[13] Dashdorj *et al.* have prepared zein/Ag composite nanofibres by dissolving zein in citric acid, ethanol and sodium hydroxide, and then adding $AgNO_3$.[16] Dippold *et al.* have demonstrated the possibility of electrospinning blends of poly(glycerol sebacate) (PGS) and zein in acetic acid solutions (15 wt.%).[17] The PGS-zein fibres were characterised by a diameter in the 300-350 nm range, a ribbon-like morphology, a tensile strength of 1.3 MPa and an elongation at break in the region of 5%. The addition of poly-L-lactic acid (PLLA) to zein was found to enhance the physical properties and has resulted in more "structurally aligned" fibres.[18] Antimicrobial nanofibres have also been produced from blends of zein with chitosan, and the compatibility of these two polymers have been increased by the addition of polyvinyl pyrrolidone (PVP).[19] Kayaci *et al*. have instead incorporated cyclodextrins as a co-polymer for zein and used dimethyl formamide as a solvent instead of conventional ethanol/water system.[20] A wide range of plasticizers, including glycerol and polyethylene glycol, have been also used for zein to enhance its mechanical properties.[21-23]

This study investigates the effect of branched polyethyleneimine (PEI) as a co-polymer for blends with zein for electrospinning of fibres, particularly in relation to the effects on the glass transition temperature (T_g) and mechanical properties of the mats produced. The novel aspects of the work are the use of PEI for the plasticization and/or toughening of zein, and the production of stable suspensions of ZnO nanoparticles within the PEI matrix (prior to the incorporation into the zein solution) by a sol-gel method based on low toxic reactants and solvents.

The sol-gel method is widely used to produce nanoparticles of metal oxides within a polymer matrix starting with a metal alkoxide or a metal carboxylate, through controlled successive steps of hydrolysis and condensation reactions.[24] Zhang *et al.* have proposed a solution mixture at 1:1:1 molar ratio of zinc acetate ($ZnAc_2$), 2-methoxyethanol (as solvent) and monoethyl amine (as micro-suspension "stabilizer" and catalyst) for sol-gel reactions leading to piezoelectric coatings.[25] Rui Zang *et al*, on the other hand, have synthesised discrete ZnO nanorods in an alcoholic sodium hydroxide solution.[26] In other works, ZnO particles were used as suspensions, omitting a final thermal treatment at high temperature. For instance, Sun *et al*. have developed a one-step hydrothermal method, inducing the required basic conditions through hexamethylenetetramine.[27] The micro suspension was stabilized with the addition of a cationic surfactant. Hong *et al.* have instead demonstrated the generation of ZnO nanoparticles in a basic aqueous solution containing polyethylene glycol as a suspension stabilizer.[28]

More recently Zinc acetyl acetonate dihydrate (ZnAc-Ac·$2H_2O$) has attracted attention as a precursor for producing ZnO nanoparticles. Ambrozic *et al.* have reported on the synthesis of ZnO nanoparticles in a neutral solution containing either 1-butanol or isobutanol as reaction medium, relying on the hydration in water to assist the decomposition of the bidendate chelate complex.[29] In the work of Brahma and Shivashankar, a microwave-assisted method has induced the conversion of Zinc acetylacetonate.phenanthroline (ZnAc-Ac.phen), which has a double tertiary amine adduct and therefore produces mild basic conditions.[30] In another work, small amounts (1-2%) of PEI have been introduced to stabilize ZnO suspensions (*ex-situ* produced) in an aqueous medium containing measured quantities of NH_4OH.[31] To the best of our knowledge, there are no reports in the literature on the *in-situ* generation of ZnO nanoparticles within a PEI matrix, which enables to bring about the required basic condition within the reaction medium, and the incorporation of these in zein fibres.

2. Method and experimental procedure

2.1. In-situ production of ZnO micro-suspensions

The production of micro-suspensions of ZnO nanoparticles within a matrix of branched PEI was carried out according to the procedure described below. The PEI used is grade b-25 kDa (Mn = 10000 Da; Mw = 25000 Da), obtained from Sigma Aldrich, which can be identified with the empirical formula $[CH_2\text{-}CH_2)_{11}(NH_2)_4(NH)_3N_4]_n$, where n~20. This can be schematically represented with a graphical structure where each repeating unit contains short linear and bifurcated branches with terminal NH_2 groups, as shown in Scheme 1. From an estimated molecular weight value for repeating unit equal to 514, the calculated NH_2 functionality comes to 82 for a degree of polymerization n = 20.

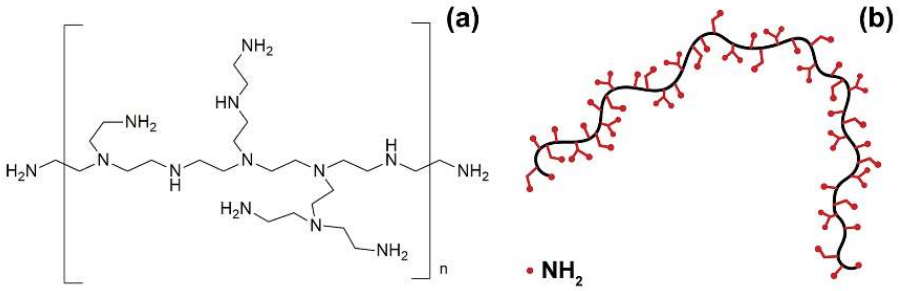

Scheme 1. Pictorial representation of (a) chemical structure (b) and chain length for the average molecular of PEI (b-25 kDa).

Zinc acetyl acetonate dihydrate ($ZnAcAc\cdot 2H_2O$) was obtained from Sigma Aldrich. It was chosen instead of $ZnAc_2$, because of the intrinsic lower acidity of the by-products, primarily acetyl acetone, which would reduce the risk of possible side effects arising from reactions with the amine groups in PEI. The reaction between Zinc acetyl acetonate dihydrate and PEI is expected to take place according to the following:

$(CH_3CO{=}CHCOCH_3)_2Zn\cdot 2H_2O = 2\ CH_3COCH_2COCH_3 + ZnO + H_2O$

From the molecular weight of $ZnAcAc\cdot 2H_2O$ and a functionality = 2, the conversion weight ratio $ZnAcAc\cdot 2H_2O$:ZnO is estimated at 3.7:1.0.

The *in-situ* production of ZnO nanoparticles within the PEI matrix at NH_2: Zn = 2:1 and NH_2: Zn = 1:1 was conducted by initially dispersing 0.75 g of zinc acetylacetonate dihydrate in 30 ml of ethanol at room temperature and mechanical stirring to form a milky suspension. The ZnO quantity for the two systems were derived from practical considerations in relation to the stability of the resulting micro-suspensions in the alcohol/PEI solution. Larger amount would

have produced excessive sedimentation due to the high density of ZnO (5.61 g/cm^3). Subsequently, a 2.5 w/v% PEI/ethanol solution was mixed with ZnAc-Ac·2H_2O at the two NH_2: Zn ratios indicated earlier and then heated up to 80 ºC under gentle mixing for 16 hours. After reaction, the suspensions were dried in polytetrafluoroethylene evaporating dishes (Cowie Technology^{TM}) under fume hood for 72 hours at room temperature to remove the solvent. Control experiments carried out using a cloudy solution of ZnAcAc·2H_2O in ethanol, without PEI, under the same reaction conditions have shown that the formation of ZnO crystals occurred at a dramatically lower degree of conversion and that the formed crystals are highly agglomerated.

The formation of ZnO particles within the PEI matrix is expected to take place through successive steps, namely (i) decomplexation of ZnAcAc·2H_2O, due to its intrinsic instability, comprising the formation of soluble intermediates; (ii) the nucleation and growth of ZnO nanoparticles, according to Scheme 2. The conversion to ZnO occurs at faster rate due to the basic environment conditions provided by the multitude of accessible NH_2 groups in the PEI. The formation of unstable soluble intermediate products provides the required conditions for a self-assembling of hydrated ZnO nuclei into a spatial configuration favourable for the formation of stable Wurtzite crystals, through stacking sequences into a tetrahedral geometry for the growth into structurally stable hexagonal faced platelets. It should be noted, however, that the high density of ZnO crystals makes it very difficult to obtain stable suspensions in a liquid medium of much lower density unless there are strong interfacial interactions. This is the reason for choosing a multifunctional polyamine as the matrix medium for the resulting micro-suspension.

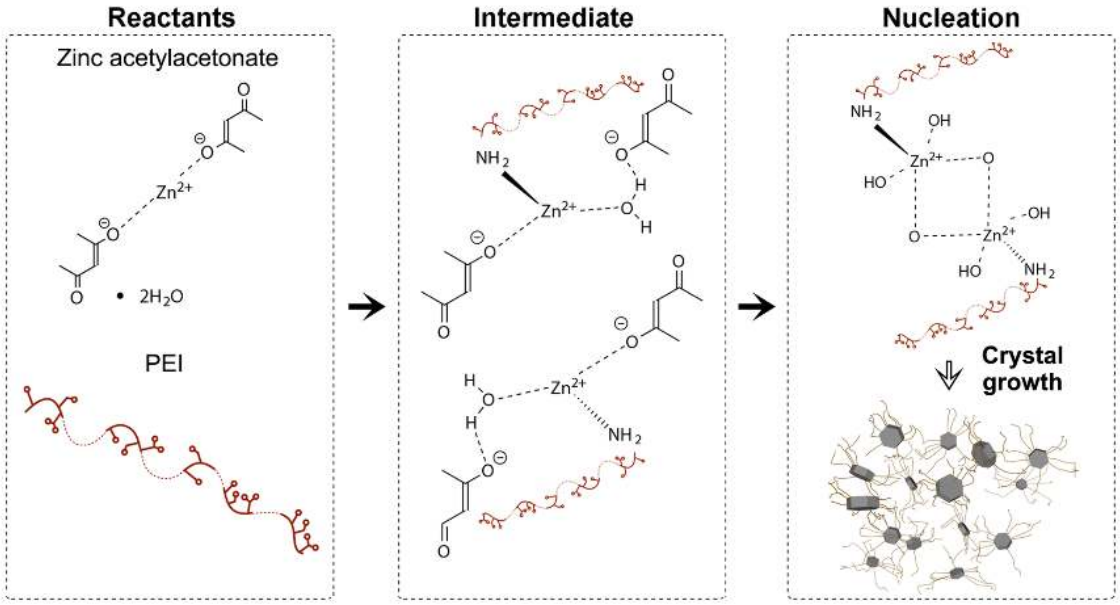

Scheme 2. Schematic illustration of the production of ZnO nanoparticles within the PEI matrix.

2.2. Electrospinning of zein/PEI/ZnO nanocomposite fibres

Zein solution mixtures were prepared at 3:1 weight ratio with PEI and PEI/ZnO micro-suspensions by mixing the components at room temperature and then adding an ethanol/water solvent mixture (7/3 v/v ratio) to produce 30 w/v% solutions. A 30 w/v% solution of zein in ethanol/water (7/3 v/v) was also prepared and used as the main control system. The electrospinning process was carried out at room temperature with an apparatus manufactured by Linari Engineering, which was run under an applied voltage of 18 kV and a flow rate of 1 ml/h and setting the tip-to-collector distance from the end of the needle at 15 cm. The syringes used have a 1 mL capacity with a 21G needle, 80 mm long and a bore diameter of 0.6 mm, which sets the exit velocity for the jet at around 0.4 mm/s. After the complete removal of water and ethanol, the theoretical content of ZnO in the fibres at full conversion is estimated to be 2.80 and 4.15 w%, based on the expectation that the acetylacetone formed as by-product remains dissolved in the fibres due to its low volatility (boiling point = 140 °C).

2.3. Electron-microscopy examinations of ZnO micro-suspensions and electrospun fibres

Field emission scanning electron microscopy (FE-SEM, Jeol 7800 and Jeol JSM-7500F) was used to study the morphology of both the ZnO /PEI micro-suspensions and the electrospun fibres with an applied voltage of 5 kV. In the case of the Jeol JSM-7500F, the electrospun fibres were carbon coated using an Emitech K950X high vacuum turbo system (Quorum Technologies Ltd, East Sussex - UK). In order to detect the ZnO particles within the fibres, a

retractable backscattered electron detector (RBEI) was used. An INLENS-SEM (LEO1530VP) was used to obtain clearer images of ZnO particles at 10 kV. The samples were coated with Au/Pb for 60s using an Emitech SC7640 sputter coater. The fibres size was measured using ImageJ software (US National Institutes of Health). For each sample, ten SEM micrographs with different magnification were analysed and 100 measurements were used to perform statistical analysis.

2.4. FTIR and XRD characterization of ZnO nanoparticles dispersed within the PEI matrix

Fourier transform infrared analysis (IR Tracer-100, Shimadzu) was carried out to monitor changes in the chemical structure of PEI/ZnO dispersions, using coatings deposited on KBR discs from the solutions and micro-dispersions. All spectra were recorded within the range 4000-1000 cm^{-1}.

Wide angle X-ray diffraction (XRD, D2 Phaser, Bruker) was used in the 2θ range of 20° to 70° to determine the presence of ZnO in the micro-suspensions. The applied voltage and the CuKα radiation were set at 20 kV and 8.04 keV respectively, using a wavelength of 0.154 nm.

2.6. Evaluation of thermal and mechanical properties of the composites

Thermogravimetric analysis (TGA) of the fibre mats in the "as produced" state was conducted in a nitrogen atmosphere, from room temperature (25 ºC) to 800 ºC with a heating rate at 10 °C/min. Approximately 10 mg of each type of mat was used.

Thermal characterisation of the fibres in the mats produced was conducted using differential scanning calorimetry (DSC Q200, TA Instruments Calorimetric Analyser) in a nitrogen atmosphere with a flow rate of 50 ml/min. Approximately 9 mg of each type of mat was sealed in an aluminium pan and subjected to a heating-cooling-heating cycle from 0 to 200 °C at 10 °C/min. Empty aluminium pans were used as reference. Data were analysed using the TA universal analysis software. All the reported values are the average of 3 samples.

The mechanical properties of the composites were investigated by tensile tests using a single column table top Instron at room temperature. The samples were cut in rectangular strips 4 mm wide and 20 mm long. The rate of extension was set at 10 mm/minute. Side action grip clamps with flat jaw faces were used.

2.7 Antibacterial tests

The antibacterial properties of fibres produced from mixtures of PEI and ZnO/PEI micro-suspensions in zein were tested on the Gram-negative bacterium *Escherichia coli* (*E. coli*) was

cultured at 37 °C in LB-Broth. The bacterial suspension was then diluted to reach 1 O.D. and 100 µl of this suspension was spread onto 10 cm^2 LB-Agar plates. Five uniform disks of fibre mats (1 cm in diameter) were prepared and sterilized for 1h under UV light. Sample-disks were hydrated using LB-Broth and gently placed on the surface of agar plates and incubated overnight at 37 °C. The inhibition zone around each disk was measured using the Fiji software.

3. Results and Discussion

3.1 PEI/ZnO dispersions

ZnO nanoparticles were synthesised *in situ* within the PEI matrix using two different NH_2:Zn ratios: 2:1 (samples indicated as PEI/ZnO-0.5) and 1:1 (samples indicated as PEI/ZnO-1.0). The reaction products were dried for 48 hours in a fume cupboard to collect the solvent free micro-suspensions of ZnO nanoparticles in PEI for characterization. SEM micrographs show that the ZnO nanoparticles in PEI/ZnO-0.5 samples have a spherical shape, while those in PEI/ZnO-1.0 samples are irregular with a higher incidence of larger agglomerates (Figure S1). Control synthesis experiments were conducted in ethanol without PEI at ZnAcAc·$2H_2O$ concentration equivalent to that used to obtain the higher ZnO content in the PEI matrix, under the same conditions (i.e. heating for 16 hours at 80 °C). SEM investigations demonstrate that only few ZnO particles are formed from the original ZnAcAc·$2H_2O$, and large crystals are due to recrystallization while drying the reaction products at room temperature (Figure S2).

The FTIR spectra of the PEI/ZnO dispersions show that a shift to lower wave numbers for the characteristic peaks of PEI (1668 and 1595 cm^{-1}) takes place when ZnO is synthesized (Figure 1a). The PEI/ZnO-0.5 and PEI/ZnO-1.0 samples exhibit peaks at 1648 and 1556 cm^{-1}. These data can be taken as evidence for the presumed interfacial interactions in accordance with the mechanism outlined in Scheme 2, supported by data reported by other authors on comparable systems. Similar interactions of NH_2 groups have been identified for polyacryloamide with $Zn(OH)_2$, where a corresponding shift was observed in the absorption peak from 1610 cm^{-1} to 1600 cm^{-1}.[31] For a composite containing ZnO nanoparticles dispersed in a matrix of polypyrrole and chitosan, a downward shift has been noted from 1708 cm^{-1} to 1654 cm^{-1}, which was also attributed to interfacial interactions.[32] The systems of the present study are closer to the first example insofar. It can be argued that, under the basic conditions imposed by the presence of PEI (pH around 10-12), the surface layers of ZnO contain large proportions of hydrated negatively charged zinc hydroxide moieties, such as $Zn(OH)_3^-$.[33] These surface ions are

expected to produce ionic interactions with the slightly positively charged -NH_2 groups within the short branches along the backbone chains of PEI. It should also be noted that the expected peak at 1716 cm^{-1} for the C=O band in ZnAcAc has not been identified in the spectra of either micro-suspensions.

XRD diffractograms of the PEI/ZnO micro-dispersions (Figure 1b) show diffraction peaks at 32.0, 34.6, 36.5, 56.7, 63.0, and 67.6° for PEI/ZnO-0.5 samples (pink curve), and at 31.4, 34.0, 35.8, 47.1, 56.2, 62.3, and 67.6° for PEI/ZnO-1.0 samples (violet curve). These peaks correspond to the planes (100), (002), (101), (102) (missing in low concentration sample),

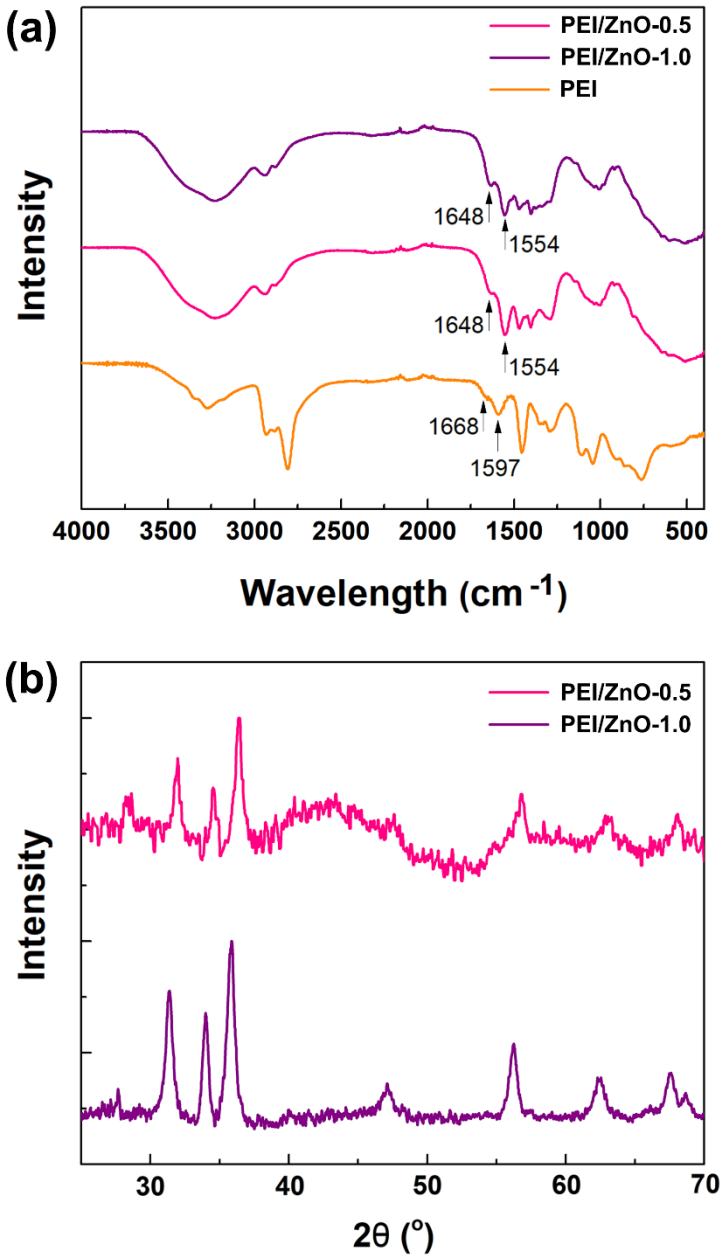

Figure 1. (a) FTIR spectra of PEI (orange curve), PEI/ZnO-0.5 micro-dispersion (pink curve) and PEI/ZnO-1.0 micro-dispersion (violet curve); (b) XRD spectra of ZnO/PEI-0.5 micro-dispersion (pink curve) and ZnO/PEI-1.0 micro-dispersion (violet curve).

(110), (103), (112), which are assigned to the hexagonal Wurtzite-type ZnO crystallographic structure.[30] The missing of (102) peak for PEI/ZnO-0.5 samples results from the submergence of the peak within the background noise, due to the presence of large amounts of the amorphous PEI matrix.

3.2 Zein/PEI/ZnO electrospun fibres

Fibres were electrospun from zein solutions, zein and PEI mixtures, zein and PEI/ZnO-0.5 (samples indicated as zein/PEI/ZnO-0.5) mixtures, and zein and PEI/ZnO-1.0 (samples indicated as zein/PEI/ZnO-1.0) mixtures. All fibres were free of beads and displayed an average diameter of (1.6±0.4), (0.7±0.2), (1.0±0.3) and (1.2±0.3) μm for zein (Figure 2a), zein/PEI (Figure 2b), zein/PEI/ZnO-0.5 (Figure 2c) and zein/PEI/ZnO-1.0 (Figure 2d), respectively. Notably, the lowest fibre diameter was exhibited by the zein/PEI fibres followed by the zein/PEI/ZnO-0.5 fibres. This could be affected by the expected lower viscosity of the spinning solutions, which would have a similar effect through an enhanced fibre splaying mechanism.[34] In addition, the shape of the cross-sectional area of the different types of fibres varied considerably. Zein fibres were ribbon-shaped, due to the formation of a rigid skin during the rapid evaporation of the solvent in the outer layers of the jet.[13,17] This prevented the occurrence of a homogeneous shrinkage with further evaporation solvent from the inner sections and caused the original circular cross section to become elliptical and then flat as a way of accommodating the reduction in cross-section area without further reduction in the perimeter. It is interesting to note that the incorporation of PEI in zein gave rise to the formation of fibres more cylindrical in shape, while the presence of ZnO nanoparticle as PEI micro-suspensions in the fibres tended to reverse this feature to a ribbon-shaped cross-section. The SEM micrograph for the zein/PEI fibres reveals also the high incidence of splays connecting adjacent fibres. Previous studies on the electrospinning of polycaprolactone (PCL) fibres containing ZnO nanoparticles have suggested that low concentrations of ZnO nanoparticles could assist the accumulation of charges on the surface of the jet, thereby decreasing the fibre diameter and narrowing the size distribution.[35] Higher ZnO concentrations (over 1%) gave rise to the formation of fibres with larger diameter, which was attributed to the agglomeration of nanoparticles. However, the agglomeration of particles can also be expected to have the opposite effect through a concomitant reduction in the viscosity of the fluid, which can in turn reduce the incidence of splays during fibre formation.[34, 35]

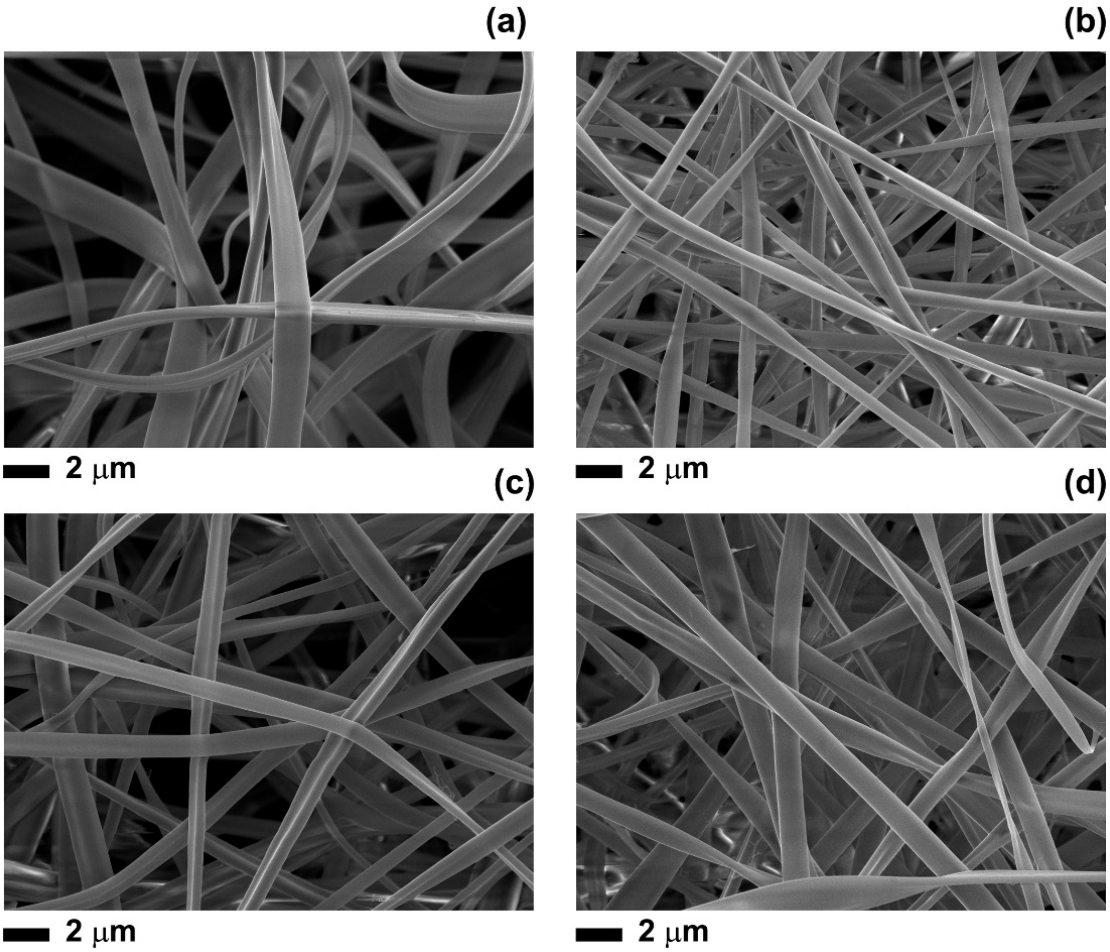

Figure 2. SEM micrographs of electrospun fibres of (a) zein, (b) zein/PEI, (c) zein/PEI/ZnO-0.5, (d) zein/PEI/ZnO-1.0.

The high magnification SEM images in Figure 3a and 3b show the presence of ZnO particles and aggregates (bright spots) distributed inside the zein/PEI/ZnO-1.0 fibres. The low density of particles can be attributed to the large discrepancy in the density between the two phases of the diluted polymer solutions, as identified also by other authors for the electrospinning of fibres based on PCL.[36]

The produced fibrous materials were analysed by TGA (Figure 3c and 3d). The initial weight loss at temperatures up to about 100 °C, due to the evaporation of residual solvent, and the subsequent plateau at temperatures in the region of 200-250 °C both increased with the amount of PEI present in the fibres. The starting point of first decomposition step of all electrospun fibres occurred at around 250 °C (derivative TGA curves). For the electrospun zein fibres the first rate of decomposition peak was found at 321 °C. The addition of PEI to zein caused this peak to become broader and to shift towards lower temperatures. Since the incorporation of ZnO nanoparticles did not change the position of these two peaks, the presence of ZnO

encapsulated in a PEI-rich matrix had no effect on the thermal decomposition kinetics of the fibres under anaerobic conditions. Accordingly, the reduction in loss of volatiles at temperatures above 350 °C for zein/PEI/ZnO-1.0 fibres can be attributed to obstacles imposed to the diffusion of volatiles by the ZnO particles, which is a typical behaviour displayed by nanocomposites.[24] This explanation is supported by the observation that the residue at 800 °C (not shown) for zein/PEI/ZnO-1.0 fibres was ~ 9 w%. The corresponding residue for the fibres obtained from either neat zein, zein/PEI blend (i.e. without ZnO) or zein/PEI/ZnO-0.5 fibres was, in all cases, in the region of 3-5 w%. This indicates that the amount and dimensions of ZnO particles in the latter systems are below the critical values required for providing an efficient barrier for the outer diffusion of volatile resulting from the chemical degradation of the polymer matrix. Furthermore, very small particles (nanoscale dimensions) may be carried away with the volatiles rather than becoming entrapped in the residue.

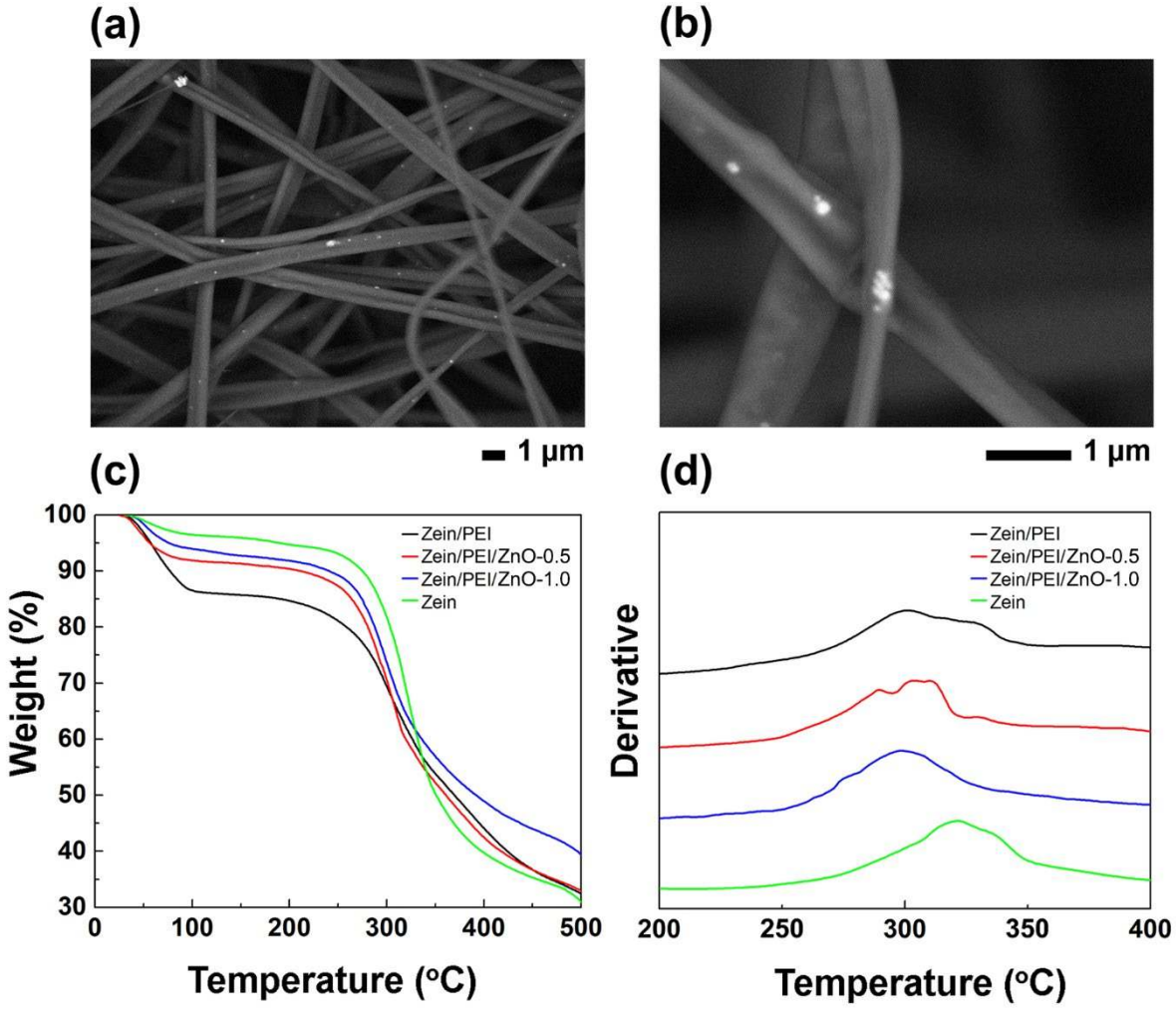

Figure 3. (a, b) High magnification SEM images of zein/PEI/ZnO-1.0 fibres. TGA thermograms for (c) weight and (d) derivative weight/time of zein/PEI (black curve), zein/PEI/ZnO-0.5 (red curve), zein/PEI/ZnO-1.0 (blue curve) and zein (green curve) electrospun fibres.

The thermograms for the 2nd cycle of DSC runs on fibres made from solutions of both zein and zein mixture with PEI as well as for the two micro-suspensions of ZnO in PEI are shown in Figure 4. The DSC traces for 1st cycle run displayed the usual broad endotherm below 100 °C due to the loss of residual solvent in the fibres.[37] The possible effect of residual water remaining from the electrospinning of the fibres has been investigated by carrying out DSC runs on fibres dried for 30 minutes at 80 °C (inset of Figure 4). The DSC thermograms show that PEI had a plasticization effect on zein, due to the strong interactions of NH_2 groups in PEI with the COOH groups of the constituent amino acids. Zein/PEI/ZnO-0.5 and zein/PEI/ZnO-1.0 fibres exhibited not only higher glass transition temperatures, due to the lower PEI content, but also a narrower transition range, which is analogous to the behaviour of zein fibres. The presence of ZnO restored part of the small endotherm at the upper end of the glass transition which was exhibited by the unmodified zein fibres. This is associated with the erasing of physical ageing, which is a behaviour often found in DSC scans of glassy polymers.[38] At the same time, an increase in the gradient of the DSC trace before the onset of the glass transition can be noted for the samples containing only PEI and the total disappearance of the physical ageing feature. The broadening of the glass transition of the zein/PEI system can be attributed to different factors: the molecular weight (MW) distribution of PEI, whereby the low molecular weight species produce a larger decrease in T_g than the corresponding high MW species; the state of aggregation of the constituents of zein.[38, 39] The narrowing of the glass transition and the significant increase in T_g resulting from the incorporation of ZnO nanoparticles is likely to arise primarily from the reduced miscibility of PEI that is attributed to presence of residual acetylacetone in the *in-situ* produced micro-suspensions. The glass transition temperature values, taken at the transition "mid-point" of the DSC traces, are 165.1±1.8 °C for zein, 129.1±5.0 °C for zein/PEI, 147.8±1.9 °C for zein/PEI/ZnO-0.5 and 160.6±1.0 °C for zein/PEI/ZnO-1.0.

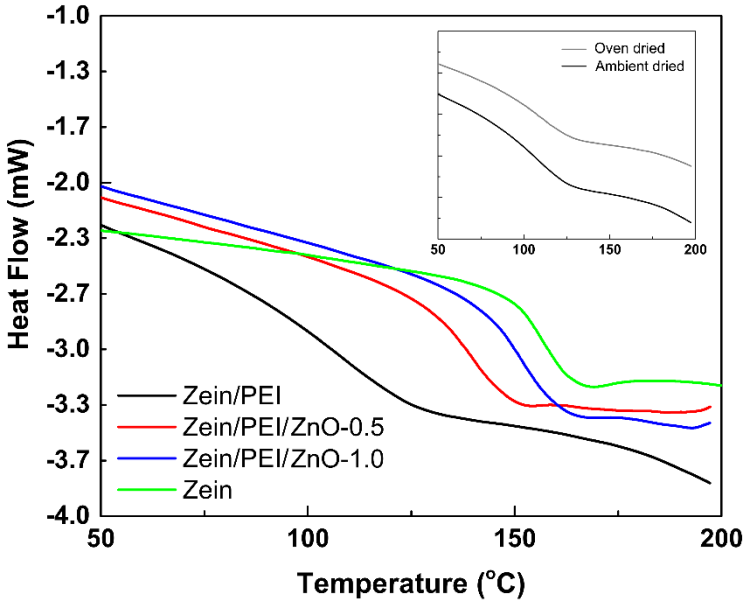

Figure 4. DSC thermograms for 2nd cycle scan on fibres of different composition with inset to compare the effect of pre-drying the fibres.

The comparison of typical stress/elongation relationship for the various systems examined are presented in Figure 5. Tests on fibres produced from pure zein solutions were not carried out as the mats were too fragile to handle. Zein/PEI/ZnO-0.5 fibre mats was found to exhibit the lowest scatter in the stress-extension curves, while zein/PEI/ZnO-1.0 fibre system was characterised by a much higher ductility, which can also be associated with the higher compliance of the mats (low gradient of the stress-extension curve). The elongation values at maximum stress and at break were both higher when ZnO particles were present in the fibres, particularly for the highest ZnO system (Figure 5b). The implications of this observation are that, although fracture occurs at lower tensile loads in the presence of ZnO nanoparticles, the high extension allows the mats to bend over larger angles without fracture. The behaviour displayed by this system would be beneficial for applications requiring easily tearing mats, which would be supported by external fastening such as microporous tapes.

Previous works on electrospun fibres of zein/collagen (3:1 ratio)[40] and zein/gelatine (3:1 ratio)[41] have reported values of yield stress of 0.2 and 0.7 MPa, respectively, which are within the same range as the values obtained for zein/PEI and zein/PEI-ZnO fibres (0.2-1.0 MPa, Table 1). Values of strain at break from 2.5 to 20.0%, as for the zein/PEI composite and nanocomposite fibres, have been registered for most of the zein-based electrospun mats, such as zein/glycerol,[42] zein/poly(glycerol sebacate),[43] zein/ethyl cellulose,[44] zein/silk fibroin,[45] zein/poly(3-hydroxybutyrate-co-4-hydroxybutyrate) (P(3HB-co-4HB)).[46]

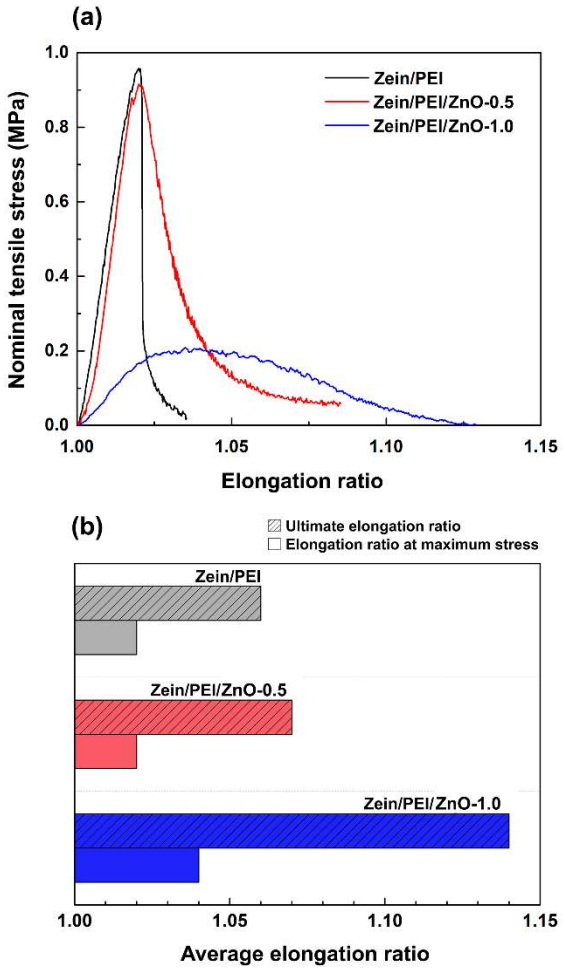

Figure 5. (a) Selected tensile curves for zein/PEI (black curve), zein/PEI/ZnO-0.5 (red curve) and zein/PEI/ZnO-1.0 (blue curve) fibres. (b) Comparison between ultimate elongation ratio and elongation ratio at maximum stress for zein/PEI (black histograms), zein/PEI/ZnO-0.5 (red histograms) and zein/PEI/ZnO-1.0 (blue histograms) fibres. Estimated error from repeated measurements is ±0.02.

Table 1: Comparison of mechanical property data for zein-based fibres produced in different studies. ε_b: elongation at break; TS: tensile strength.

Fibres	ε_b (%)	TS (MPa)	Experimental parameters	Ref.
Zein/poly(glycerol sebacate) (3:1 ratio)	6	2.2	Polymer concentration: 30% w/v. Solvents: acetic acid and ethanol. E-spin: 20 kV, 0.4-07 mL/h, 10-15 cm.	42
Zein/poly(glycerol sebacate) (6:1 ratio)	10	1.0		
Zein/ethyl cellulose (3:1 ratio)	12	3.5	Polymer concentration: 40% w/v. Solvent: acetic acid. E-spin: 18 kV, 0.5 mL/h, 15 cm.	44
Zein/ethyl cellulose (1:1 ratio)	8	6.0		
Zein/silk fibroin (2:1 ratio)	25	14	Polymer concentration: higher than 25% w/v. Solvent: formic acid. E-spin: 14-16 kV, 6 mL/h, 12 cm.	45
Zein/silk fibroin (1:1 ratio)	15	14		
Zein/P(3HB-co-4HB) (3:2 ratio)	20	5.4	Polymer concentration: 5% w/v. Solvent: dimethylformamide. E-spin: 26 kV, 0.2 mL/h, 20 cm.	46
Zein/P(3HB-co-4HB) (2:3 ratio)	46	6.4		
Zein/collagen (3:1 ratio)	40	0.2	Polymer concentration: 40% w/v. Solvent: acetic acid. E-spin: 20 kV, 0.75 mL/h, 15 cm.	40
Zein/collagen (1:1 ratio)	15	4.0		
Zein/gelatine (3:1 ratio)	88	0.7	Polymer concentration: 30% w/v. Solvent: acetic acid. E-spin: 15 kV, 1 mL/h, 10 cm.	41
Zein/gelatine (2:1 ratio)	69	0.3		
Zein/gelatine (1:1 ratio)	8	0.8		
Zein/PEI (3:1 ratio)	6	1.0	Polymer concentration: 30% w/v. Solvents: ethanol/water (7/3). E-spin: 18 kV, 1 mL/h, 15 cm.	This study
Zein/PEI-ZnO-0.5 (3:1 ratio)	7	0.8		
Zein/PEI-ZnO-1.0 (3:1 ratio)	14	0.2		

The presence of the ZnO nanoparticles conferred antibacterial properties to the zein/PEI electrospun mats. *In vitro* tests on bacteria proliferation exhibited a clear inhibition zone (0.8±0.1 cm) in the areas below and around the zein/PEI-ZnO samples (Figure 6). This was not visible for the zein/PEI mats without ZnO. It should be noted that the bactericidal properties of ZnO nanoparticles have been extensively investigated in the literature,[47] however only few groups have incorporated ZnO nanoparticles into zein-based materials and none have until now used an *in-situ* generation method to produce solution mixtures for electrospinning of fibres. For instance, Cao and co-workers have reported on zein films containing spindle-like zein-conjugated ZnO crystals and ZnO rods, both produced *ex situ*.[48, 49] The films with 1.8-4.4 μg/mm^2 of ZnO were able to inhibit the proliferation of *E. coli* and *Staphyloccocus aureus*.

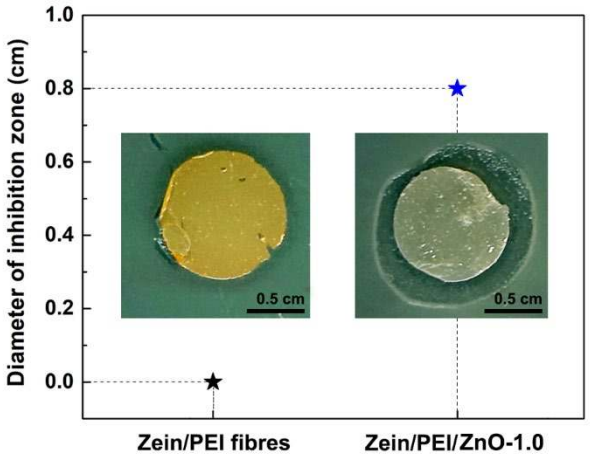

Figure 6. Size of the inhibition zone for *E. coli* colonies in contact with zein/PEI and zein/PEI/ZnO-1.0 electrospun mat. Inset: photographs of zein/PEI (left-hand side) and zein/PEI/ZnO-1.0 (right-hand side) samples.

Although the exact mechanism of action of ZnO nanoparticles against microorganisms has not been clarified yet, the possible explanations for the antimicrobial activity of ZnO can be attributed to the following: a) the nanoparticles accumulation on the bacterial exterior that results in membrane perturbation, with changes in permeability and ultimately the disruption of the cell integrity; b) the release of Zn^{2+} ions that leads to inhibition of active transport and has severe impact on the amino acid metabolism and the enzyme system; c) the generation of reactive oxygen species that destroy several cellular components (lipids, DNA and proteins).[47] For the system of this study the surface of ZnO crystals are expected to be very rich in Zn^{2+} ions due to strong associations with NH_2 groups in the surrounding PEI (see Scheme 2) and in accordance to the findings by Tang *et al.*[33] It is worth noting that the data in a report by Soria-Castro *et al.* found that mixed Ca/Zn hydroxides displayed antimicrobial properties and suggested that $Zn(OH)_2$ alone may not have such characteristics.[50] Other authors found that mixed zinc oxide/zinc hydroxide nanoparticles exhibit antimicrobial activity against *E. coli* and *S. aureus*.[51] For the interpretation of the results of this study it is propitious to consider also the findings of Malzahan *et al.* on plasma-polymerized thin films deposited from zinc acetylacetonate in a low-pressure RF plasma reactor.[52] These authors have obtained a sixfold reduction in the growth of *S. aureus* on films of different thickness, which was attributed to the presence of complexes of ZnO and ZnAcAc. This interpretation reinforces the hypothesis on the existence of the intermediate structure identified in Scheme 2.

4. Conclusions

Experiments were carried out with the view of producing novel zein based fibres by electrospinning. Polyethyleneimine (PEI) was used for its dual function, namely as a potential plasticizer for zein and as favourable medium for the *in-situ* generation of ZnO nanoparticles. Zinc acetyl acetonate dihydrate ($ZnAcAc.2H_2O$) was chosen as the owing to its low stability, which facilitates the formation of ZnO through successive sol-gel reaction steps, consisting of decomplexation of $ZnAcAc.2H_2O$, formation of solid nuclei and growth into stable Wurtzite crystals. The obtained ZnO/PEI micro-suspension in ethanol was mixed in an ethanol/water solution of zein at two concentration levels and used to electrospin different types of zein-modified fibres. ZnO micro-suspensions and the zein-based fibres were characterised and evaluated. The use of PEI in the production of ZnO nanoparticles was found to facilitate the conversion, owing to the basic environment of the reaction medium. XRD examination has confirmed the crystallographic structure of the ZnO particles formed, while SEM examinations showed the formation of agglomerates less than 400 nm made up of much smaller primary nanoparticles. FTIR spectroscopic analysis has indicated that the amine groups in PEI can strongly interact with the surface of ZnO crystals, possibly through associations with ionic species, such as $Zn(OH)_3^-$, arising from the basic nature of the suspension medium.

DSC analysis has revealed that PEI acts as an "effective" plasticizer for zein, causing also a broadening of the glass transition. However, when ZnO nanoparticles are concomitantly present in the solution mixture used in making the fibres the extent of plasticization, expressed as a decrease of the T_g value, is reduced and the narrower breath of the glass transition exhibited by the "neat" zein fibres is restored. TGA data have shown that the presence of PEI increases the solvent retention of the fibres produced, which is reduced considerably when ZnO nanoparticles are present as a micro-suspension in PEI.

It has also been found that the structural modifications of zein, brought about by the addition of PEI and ZnO/PEI micro-suspensions, affects both the shapes and diameter of the fibres produced. The incorporation of PEI in the zein spinning solution results in a significant reduction in fibre diameter, as well as producing fibres with a more cylindrical cross-section relative to the fibres produced from mono-component zein solution, which have a ribbon type shape due to the formation of a "hard" and impermeable skin in the first stage of the solvent evaporation from the spinning jet.

The mats containing ZnO nanoparticles were found to exhibit antibacterial properties, manifest by the formation of the inhibition zone for *E. coli* colonies, likely resulting from the formation of ZnO complexes with Zinc acetylacetone as intermediate or side products of the sol-gel

reactions. For the systems of this study there are various foreseen potential applications that would combine the antibacterial properties provided by presence of ZnO nanoparticles with the release of drugs entrapped on the surface of the fibres through associations with the amine groups of PEI. This would provide the means of controlling the rate of release through variations in the concentration of PEI in the fibres and the composition of auxiliary components that may be used as carriers in the interstices between the fibres of the mats. Examples are dressings and membranes for biomedical applications and food industry.

Acknowledgements

FG and PPP thank D. Guarnieri for the useful discussions. EM thanks the Rosetrees Trust for financial support (Grant JS16/M715). WZ thanks C. Protheroe for software technical support.

Supporting Information

SEM images of ZnO/PEI micro-dispersions.

References

(1) Shukla, R.; Cheryan, M. Zein: the industrial protein from corn. *Ind. Crops Prod.* **2001**, *13*, 171-192

(2) Zhang, Y.; Cui, L.; Li, F.; Shi, N.; Kong, W. Design, fabrication and biomedical applications of zein-based nano/micro-carrier systems. *Int. J. Pharma.* **2016**, *513*, 191-210.

(3) Demir, M.; Ramos-Rivera, L.; Silva, R.; Nazhat, N. S.; Boccaccini, A. R. Zein-based composites in biomedical applications. *J. Biom. Mater. Res.-Part A* **2017**, *105*, 1656-1665.

(4) Yong, Z.; Lili, C.; Xiaoxia, C.; Heng, Z.; Nianqiu, S.; Chunlei, L.; Yana, C.; Wei, K. Zein-based films and their usage for controlled. *J. Control. Rel.* **2015**, *206*, 206-219.

(5) Torres-Giner, S.; Gimenez, E.; Lagaron, J. M. Characterization of the morphology and thermal properties of Zein Prolamine nanostructures obtained by electrospinning. *Food Hydrocoll.* **2008**, *22*, 601-614.

(6) Karthikeyan, K.; Shoba, E.; Janani, I.; Poornima, B.; Purna Sai, K. Electrospun protein nanofibers in healthcare: A review. *Int. J. Pharma.* **2007**, *523*, 552-590.

(7) Dias Antunes, M.; da Silva Dannenberg, G.; Fiorentini, A. M.; Pinto V. Z.; Lim, L. T.; da Rosa Zavarese, E.; Dias, A. R. G. Antimicrobial electrospun ultrafine fibers from zein containing eucalyptus essential oil/cyclodextrin inclusion complex. *Int. J. Biol. Macromol.* **2017**, *104*, 874-882.

(8) Acevedo, F.; Hermosilla, J.; Sanhueza, C.; Mora-Lagos, B.; Fuentes, I.; Rubilar, M.; Concheiro, A.; Alvarez-Lorenzo, C. Gallic acid loaded PEO-core/zein-shell nanofibers for chemopreventive action on gallbladder cancer cells. *Eu. J. Pharma. Sci.* **2018**, *119*, 49-61.
(9) Wang, H.; Hao, L.; Wang, P.; Chen, M.; Jiang, S.; Jiang, S. Release kinetics and antibacterial activity of curcumin loaded zein fibers. *Food Hydrocoll.* **2017**, *63*, 437-446.
(10) Lu, H.; Wang, Q.; Li, G.; Qiu, Y.; Wei, Q. Electrospun water-stable zein/ethyl cellulose composite nanofiber and its drug release properties. *Mater. Sci. Eng. C* **2017**, *74*, 86-93.
(11) Karthikeyan, K.; Guhathakarta, S.; Rajaram, R.; Korrapati, P. S. Electrospun zein/eudragit nanofibers based dual drug delivery system for the simultaneous delivery of aceclofenac and pantoprazole. *Int. J. Pharma.* **2012**, *438*, 117-122.
(12) Yang, S. B.; Rabbani, M. M.; Ji, B. C.; Han D.-W.; Lee, J. S.; Kim, J. W.; Yeum, J. H. Optimum conditions for the fabrication of zein/Ag composite nanoparticles from ethanol/H_2O co-solvents using electrospinning. *Nanomaterials* **2016**, *12*, 230-241.
(13) Babitha, S.; Korrapati, P. S. Biodegradable zein-polydopamine polymeric scaffold impregnated with TiO_2 nanoparticles for skin tissue engineering. *Biomed. Mater.* **2017**, *12*, 055008.
(14) Figueira, D. R.; Miguel, S. P.; De Sá, K. D.; Correia, I. J. Production and characterization of polycaprolactone- hyaluronic acid/chitosan- zein electrospun bilayer nanofibrous membrane for tissue regeneration. *Int. J. Biol. Macromol.* **2016**, *93*, 1100-1110.
(15) Unnithan, A. R.; Gnanasekaran, G.; Sathishkumar, Y,; Lee, Y. S.; Kim, C. S. Electrospun antibacterial polyurethane–cellulose acetate–zein composite mats for wound dressing. *Carbohydr. Polym.* **2014**, *102*, 884-892.
(16) Dashdorj, U.; Reyes, M. K.; Unnithan, A. R.; Tiwari, A. P.; Tumurbaatar, B.; Park, C. H.; Kim, C. S. Fabrication and characterization of electrospun zein/Ag nanocomposite mats for wound dressing applications. *Int. J. Biol. Macromol.* **2015**, 80, 1-7.
(17) Dippold, D.; Tallawi, M.; Tansaz, S.; Roether, J. A.; Boccaccini, A. R. Novel electrospun poly(glycerol sebacate)-zein fiber mats as candidate materials for cardiac tissue engineering. *Eu. Polym. J.* **2016**, *75*, 504-513.
(18) Yao, C.; Li, X.; Song, T. Preparation and characterization of zein and zein/poly-l-lactide nanofiber yarns. *J. Appl. Polym. Sci.* **2009**, *114*, 2079-2086.
(19) Torres-Giner, S.; Ocio, M. J.; Lagaron, J. M. Novel antimicrobial ultrathin structures of zein/chitosan blends obtained by electrospinning. *Carbohydr. Polym*. **2009**, *77*, 261-266.
(20) Kayaci, F.; Uyar, T. Electrospun zein nanofibers incorporating cyclodextrins. *Carbohydr. Polym.* **2012**, *90*, 558-568.

(21) Emmambux, M. N.; Stading, M. In situ tensile deformation of zein films with plasticizers and filler materials. *Food Hydrocoll*. **2007**, *21*, 1245-1255.
(22) Jing, L.; Wang, X.; Liu, H.; Lu, Y.; Bian, J.; Sun, J.; Huang, D. Zein increases the cytoaffinity and biodegradability of scaffolds 3D-printed with zein and poly(ε-caprolactone) composite ink. *ACS Appl. Mater. Interfaces* **2018**, *10*, 18551-18559.
(23) Xu, H.; Chai, Y.; Zhang, G. Synergistic effect of oleic acid and glycerol on zein film plasticization. *J. Agric. Food Chem*. **2012**, *60*, 10075-10081.
(24) Mascia L. Fillers Generated *In-Situ*: Organic-Inorganic Hybrids, in "Functional Fillers for Plastics"; 2nd Edition (M. Xanthos, Editor), (2010) Wiley-VCH, ISBN 3-527-31054-1.
(25) Zhang, K.; Zhao, Y.; He, F.; Liu, D.-G. Piezoelectricity of ZnO films prepared by sol-gel method. *Chinese J. Chem. Phys.* **2007**, *20*, 721-726.
(26) Zhang, R.; Yin, P.-G.; Wang, N.; Guo, L. Photoluminescence and Raman scattering of ZnO nanorods. *Solid State Sci.* **2009**, *11*, 865-869.
(27) Sun, Y.; Guo, H.; Zhang, W.; Zhou, T.; Qiu, Y.; Xu, K.; Zhang, B.; Yang, H. Synthesis and characterization of twinned flower-like ZnO structures grown by hydrothermal methods. *Ceram. Int.* **2016**, *42*, 9648-9652.
(28) Hong, R.; Pan, T.; Qian, J.; Li, H. Synthesis and surface modification of ZnO nanoparticles. *Chem. Eng. J.* **2006**, *119*, 71-81.
(29) Ambrozic, G.; Škapin, S. D.; Zigon, M.; Orel, Z. C. The synthesis of zinc oxide nanoparticles from zinc acetylacetonate hydrate and 1-butanol or isobutanol. *J. Coll. Interf. Sci.* **2010**, *346*, 317-323.
(30) Brahma, S.; Shivashankar, S. A. Yellow-red luminescence in ZnO nanoparticles synthesized from zinc acetylacetonate phenanthroline. *Mater. Lett.* **2016**, *164*, 235-238.
(31) Susko, F. J.; Scheiner, B. J. Infrared spectroscopic study of the flocculation of zinc and copper precipitates. *Report of Investigations 9321*, United States Bureau of Mines.
(32) Ebrahimiasl, S.; Zakaria, A.; Kassim, A.; Basri, S. N. Novel conductive polypyrrole/zinc oxide/chitosan bionanocomposite: synthesis, characterization, antioxidant, and antibacterial activities. *Int. J. Nanomed.* **2015**, *10*, 217-227.
(33) Tang, F.; Uchikoshi, T.; Sakka, Y. Electrophoretic deposition behavior of aqueous nanosized zinc oxide suspensions. *J. Am. Ceram. Soc.* **2002**, *85*, 2161-2165.
(34) Mascia, L.; Su, R.; Clarke, J.; Lou, Y.; Mele, E. Fibres from blends of epoxidized natural rubber and polylactic acid by the electrospinning process: Compatibilization and surface texture. *Eu. Polym. J.* **2017**, *87*, 241-254.

(35) Koombhongse, S.; Liu, W.; Reneker, D. H. Flat polymer ribbons and other shapes by electrospinning. *J. Polym. Sci.: Part B: Polym. Phys.* **2001**, *39*, 2598-2606.
(36) Augustine, R.; Malik, H. N.; Singhal, D. K.; Mukherjee, A.; Malakar, D.; Kalarikkal, N.; Thomas, S. Electrospun polycaprolactone/ZnO nanocomposite membranes as biomaterials with antibacterial and cell adhesion properties. *J. Polym. Res.* **2014**, *21*, 347.
(37) Chen, Y.; Ye, R.; Liu, J. Effects of different concentrations of ethanol and isopropanol on physicochemical properties of zein-based films. *Ind. Crops Prod.* **2014**, *53*, 140-147.
(38) Lionetto, F.; Mascia, L.; Frigione, M. Evolution of transient-states and properties of an epoxy-silica hybrid cured at ambient temperature. *Eu. Polym. J.* 2013, 49, 1298-1313.
(39) Kim, S.; Xu, J. Aggregate formation of zein and its structural inversion in aqueous ethanol. *J. Cereal Sci.* 2008, 47, 1-5.
(40) Lin, J.; Li, C.; Zhao, Y.; Hu, J.; Zhang, L.-M. Co-electrospun nanofibrous membranes of collagen and zein for wound healing. *ACS Appl. Mater. Interfaces* **2012**, *4*, 1050-1057.
(41) Deng, L.; Zhang, X.; Li, Y.; Que, F.; Kang, X.; Liu, Y.; Feng, F.; Zhang, H. Characterization of gelatin/zein nanofibers by hybrid electrospinning. *Food Hydrocoll.* **2018**, *75*, 72-80.
(42) Wongsasulak, S.; Tongsin, P.; Intasanta, N.; Yoovidhya, T. Effect of glycerol on solution properties governing morphology, glass transition temperature, and tensile properties of electrospun zein film. *J. Appl. Polym. Sci.* **2010**, *118*, 910-919.
(43) Vogt, L.; Liverani, L.; Roether, J. A.; Boccaccini, A. R. Electrospun zein fibers incorporating poly(glycerol sebacate) for soft tissue engineering. *Nanomaterials* **2018**, *8*, 150.
(44) Lu, H.; Wang, Q.; Li, G.; Qiu, Y.; Wei, Q. Electrospun water-stable zein/ethyl cellulose composite nanofiber and its drug release properties. *Mater. Sci. Eng. C* **2017**, *74*, 86-93.
(45) Yao, C.; Li, X.; Song, T.; Li, Y.; Pu, Y. Biodegradable nanofibrous membrane of zein/silk fibroin by electrospinning. *Polym. Int.* **2009**, *58*, 396-402.
(46) Zhijiang, C.; Qin, Z.; Xianyou, S.; Yuanpei, L. Zein/poly(3-hydroxybutyrate-co-4-hydroxybutyrate) electrospun blend fiber scaffolds: Preparation, characterization and cytocompatibility. *Mater. Sci. Eng. C* **2017**, *71*, 797-806.
(47) Amna, S.; Shahrom, M.; Azman, S.; Kaus, N. H. M.; Ling Chuo, A.; Siti, K.; Mohd, B.; Habsah, H.; Dasmawati, M. Review on zinc oxide nanoparticles: antibacterial activity and toxicity mechanism. *Nano-Micro Lett*. **2015**, *7*, 219-242.
(48) Cao, Y.; Chen, T.-T.; Wang, W.; Chen, M.; Wang, H.-J. Construction and functional assessment of zein thin film incorporating spindle-like ZnO crystals. *RSC Adv.* **2017**, *7*, 2180-2185.

(49) Cao, Y.; Du, S.; Chen, T.-T.; Chen, M. Effects of inorganic antiseptic on the properties of zein-based active films. *J. Polym. Environm.* **2018**, *26*, 4430-4440.
(50) Soria-Castro, M.; de la Rosa-García, S. C.; Quintana, P.; Gómez-Cornelio, S.; Sierra-Fernandez, A.; Gómez-Ortíz, N. Broad spectrum antimicrobial activity of Ca(Zn(OH)3)2·2H2O and ZnO nanoparticles synthesized by the sol-gel method. *J. Sol-Gel Sci. Tech.* **2019**, *89*, 284-294.
(51) Zare Khafri, H.; Ghaedi, M.; Asfaram, A.; Javadian, H.; Safarpoor, M. Synthesis of CuS and ZnO/$Zn(OH)_2$ nanoparticles and their evaluation for in vitro antibacterial and antifungal activities. *Appl. Organometal Chem.* **2018**, *32*, e4398.
(52) Malzahn, K.; Duque, L.; Ciernak, P.; Wiesenmuller, S.; Bender, K.; Forch, R. Antimicrobial activity and cyto-compatibility of plasma polymerized zinc acetylacetonate thin films. *Plasma Process. Polym.* **2013**, *10*, 243-249.

Table of Contents